JMEPEG (2012) 21:1862–1872
DOI: 10.1007/s11665-011-0103-1

1059-9495/$19.00

Mathematical Modeling of Weld Bead Geometry, Quality, and Productivity for Stainless Steel Claddings Deposited by FCAW

J.H.F. Gomes, S.C. Costa, A.P. Paiva, and P.P. Balestrassi

(Submitted January 31, 2011; in revised form November 21, 2011)

In recent years, industrial settings are seeing a rise in the use of stainless steel claddings. The anti-corrosive surfaces are made from low cost materials such as carbon steel or low alloy steels. To ensure the final quality of claddings, however, it is important to know how the welding parameters affect the process's outcome. Beads should be defect free and deposited with the desired geometry, with efficiency, and with a minimal waste of material. The objective of this study then is to analyze how the flux-cored arc welding (FCAW) parameters influence geometry, productivity, and the surface quality of the stainless steel claddings. It examines AISI 1020 carbon steel cladded with 316L stainless steel. Geometry was analyzed in terms of bead width, penetration, reinforcement, and dilution. Productivity was analyzed according to deposition rate and process yield, and surface quality according to surface appearance and slag formation. The FCAW parameters chosen included the wire feed rate, voltage, welding speed, and contact-tip-workpiece distance. To analyze the parameters' influences, mathematical models were developed based on response surface methodology. The results show that all parameters were significant. The degrees of importance among them varied according to the responses of interest. What also proved to be significant was the interaction between parameters. It was found that the combined effect of two parameters significantly affected a response; even when taken individually, the two might produce little effect. Finally, the development of Pareto frontiers confirmed the existence of conflicts of interest in this process, suggesting the application of multi-objective optimization techniques to the sequence of this study.

Keywords design and analysis of experiments, flux cored arc welding, response surface methodology, stainless steel claddings, surfacing

1. Introduction

Surfacing is a welding process in which a layer of filler metal is deposited over the surface of another material to obtain desired properties or dimensions. It is generally used for three purposes to extend the useful life of a part that, for a given application, lacks needed properties; to restore elements affected by corrosion or wear; and to create surfaces with special features (Ref 1). Of these three applications, this last one, in industrial settings, is noticeably on the rise. Considering the various types of surfacing materials, stainless steel claddings are characterized as one with the most frequent applications (Ref 2). The stainless steel cladding process is then defined as the deposition of a stainless steel layer on surfaces of carbon steel or low alloy steels to produce claddings with anti-corrosion properties and resistance needed to withstand environments subjected to high wear due to corrosion. Impressive results have made the process quite attractive. Essentially, the process produces surfaces, out of common materials that are resistant to corrosive environments. This is obtained at a cost dramatically lower than using the pure, highly expensive components of stainless steel. As a result, carbon steels cladded with stainless steels are gaining stronghold in various types of industries including petroleum, chemical, food, agricultural, nuclear, naval, railway, civil construction, etc. (Ref 3, 4).

While its potential economic advantages are great, the stainless steel cladding is a complex welding process. Several input parameters and multiple response variables are involved. Thus, finding the proper control over the process parameters is essential to achieve a desired quality of the material deposited (Ref 5).

How cladding applications differ from conventional welding mainly concerns the weld bead geometry. Unlike conventional applications that require high penetration (P) to ensure the resistance of the weld (Fig. 1a), the desired weld bead geometry in cladding applications includes high bead width (W), high reinforcement (R), low penetration (P), and low dilution percentage (D) (Fig. 1b). This profile geometric characteristic that is important for the process allows covering the largest possible area with the least number of passes, resulting in significant savings of time and material.

In the cladding process, another critical aspect is the dilution control. This control, according to several researchers, is critical to ensuring the final quality of the claddings (Ref 6-8). Shahi and Pandey (Ref 9) claim that dilution strongly influences the

J.H.F. Gomes, S.C. Costa, and **A.P. Paiva**, Institute of Industrial Engineering, Federal University of Itajubá, Itajubá, Minas Gerais, Brazil; and **P.P. Balestrassi**, Institute of Industrial Engineering, Federal University of Itajubá, Itajubá, Minas Gerais, Brazil; Department of Industrial and Information Engineering, The University of Tennessee, 416 East Stadium Hall, Knoxville, TN 37996. Contact e-mails: balestrassi@ utk.edu and pedro@unifei.edu.br.

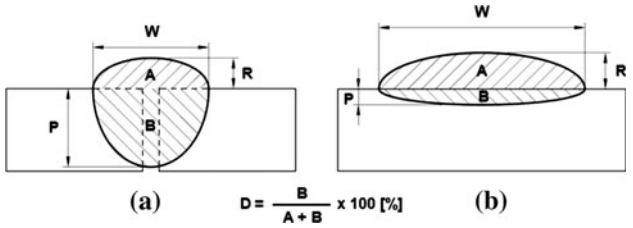

Fig. 1 Desired weld bead geometry: (a) union joint (typical applications) and (b) cladding

chemical composition and properties of cladded components. In the stainless steel cladding process, increasing the dilution reduces the alloying elements and increases the carbon content in the cladded layer, giving rise to a number of metallurgical problems. Chief among these is that the metal is less corrosion resistant. Therefore, researchers are studying and developing procedures that are able to offer an optimal dilution.

Recent years have seen the development of several studies addressing stainless steel cladding process (Ref 2-20). As this process has been increasing in industrial environments, most of the previous research studies have focused on analyzing the final properties of the claddings, checking whether the welding process used is capable of producing claddings with the required specifications to withstand conditions of high wear corrosion (Ref 10-18). The main tests evaluate the microstructure, hardness, tensile properties, and corrosion resistance. On the other hand, some studies have sought to better understand the cladding process, looking for mathematical relationships between the welding process's input parameters and the response variables (Ref 3-9). For this approach, the researchers have concerned themselves with dilution and the parameters of the weld bead geometry, analyzing how variations in process parameters influence these responses.

A review of the literature reveals two fundamental groups of researchers: those analyzing final properties and those studying the cladding's geometric characteristics. Considering the industry's current demand for efficient and economic processes, little study has been concerned with the analysis of variables related to the productivity of the process (Ref 19, 20). As was said earlier, an important factor in achieving the final quality of the claddings is control over the process. In this respect, the effects of welding parameters on the results of the cladding process are known to be related to the beads being defect free and deposited with the desired geometry, with good yield and with a minimal waste of material.

Given these theoretical considerations, this article aims to analyze how flux-cored arc welding (FCAW) parameters influence geometry, productivity, and the quality of stainless steel claddings deposited on surfaces of carbon steel. Regarding the welding parameters, we considered the effects of wire feed rate, voltage, welding speed, and contact-tip-workpiece distance (CTWD). The weld bead geometry was analyzed by the bead width, penetration, reinforcement, and dilution. Productivity included the deposition rate and process yield. Regarding quality, the slag formation and surface appearance were considered.

The choice of studying the FCAW process is justified with the advantages it has exhibited. It obtains high deposition rates, has minimal waste of electrode, shows process flexibility, produces high-weld quality, and demonstrates excellent control of the weld pool (Ref 21).

The parameters' influence was analyzed using mathematical models developed through design and analysis of experiments techniques, mainly using the response surface methodology (Ref 22-24). According to Montgomery (Ref 22), this methodology is a collection of mathematical and statistical techniques, which are useful in modeling and analyzing problems where responses of interest are affected by multiple input parameters. Such techniques have been used successfully for the analysis of welding processes by such researchers as Palani and Murugan (Ref 4), Kannan and Murugan (Ref 6), and Balasubramanian et al. (Ref 8).

2. Experimental Method

The response surface methodology was divided into four phases: (1) experiments planning; (2) experimental procedure; (3) mathematical modeling of responses of interest; and (4) analysis of parameters' influence. The steps followed in each phase are detailed in Fig. 2.

2.1 Experiments Planning

The FCAW parameters examined are wire feed rate, voltage, welding speed, and CTWD. In defining the parameters' levels, previous research, and preliminary tests were taken into account. Thus, by analyzing previous studies and considering the objectives of this study, the limits of each variable were prefixed. Then, preliminary tests were performed to find the extreme levels for each variable, thus determining whether the process occurred under such conditions. Table 1 shows the parameters and their levels, set at the end of the preliminary tests.

The responses examined include the bead width (W), penetration (P), reinforcement (R) and dilution (D), representing the weld bead geometry. The responses of productivity are the deposition rate (DR) and process yield (Y). For quality, the slag formation (SF) and the surface appearance (SA) were considered.

The experimental matrix used was the central composite design (CCD) with four factors at five levels, eight axial points, seven center points, and one replication, resulting in 31 experiments. The value adopted for α was 2.0. CCDs are often recommended when the design plan calls for sequential experimentation because these designs can incorporate information from a properly planned factorial experiment (Ref 22). The factorial and center points may serve as a preliminary stage where you can fit a first-order (linear) model, but still provide evidence regarding the importance of a second-order contribution or curvature.

2.2 Experimental Procedure

The experiments were carried out using a welding machine ESAB AristoPower 460 and a module AristoFeed 30-4W MA6, this latter one employed to feed the wire. The control of the welding speed and the torch angle were provided by a mechanical system device. The base metal used was a carbon steel AISI 1020, cut into plates of 120 mm × 60 mm × 6.35 mm. The filler metal employed was a flux-cored stainless steel wire of type AWS E316LT1-1/4, of 1.2-mm diameter. Table 2 presents the chemical composition of these materials.

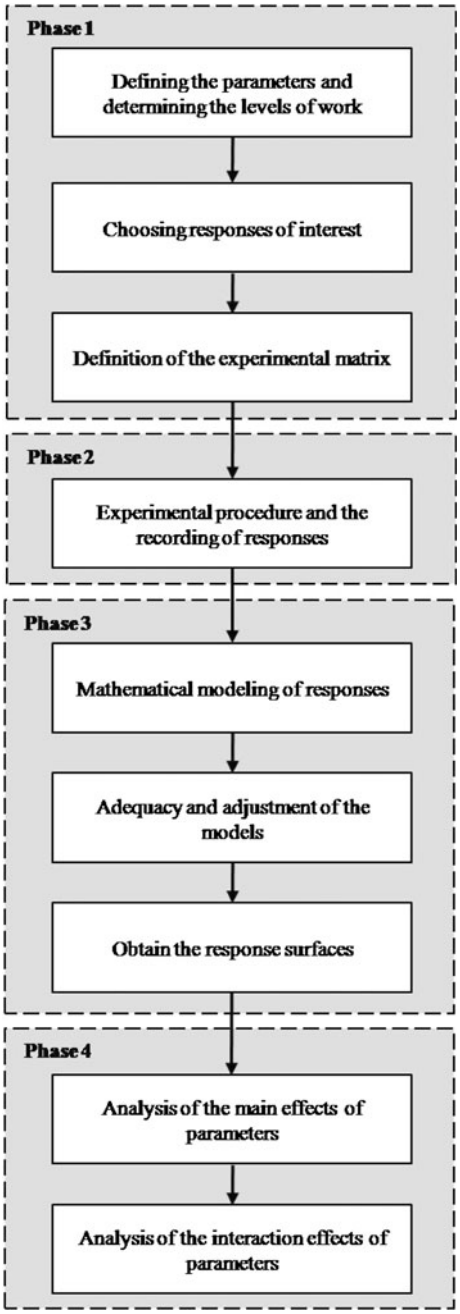

Fig. 2 Experimental method

Table 1 Parameters and their levels

Parameters	Unit	Notation	Levels				
			−2	−1	0	+1	+2
Wire feed rate	m/min	W_f	5.5	7.0	8.5	10.0	11.5
Voltage	V	V	24.5	27.0	29.5	32.0	34.5
Welding speed	cm/min	S	20	30	40	50	60
CTWD	mm	N	10	15	20	25	30

Experiments were performed by simply depositing a bead of stainless steel onto carbon steel plates (bead on plate), taking into account the parameters defined in Table 3. The shielding gas used was the mixture 75%Ar+25%CO_2 at a flow rate of 16 l/min. The torch angle was set at 15° to "pushing."

Table 2 Chemical composition of base metal and filler metal

Material	C	Mn	P	S	Si	Ni	Cr	Mo
AISI 1020	0.18/0.23	0.30/0.60	0.04	0.05	…	…	…	…
E316LT1-1/4	0.03	1.58	…	…	1.00	12.4	18.5	2.46

Recording the responses was made in three steps:

(1) Evaluation of the quality: researchers evaluated both the slag formation and the surface appearance by assigning them scores. The slag formation (SF) was scored from 1 to 5 on the following basis:

1: bad slag formation, uneven and flawed;
2: slag formation with large failures in the coating;
3: slag formation with some areas not covered;
4: slag formation with minor flaws in the coating;
5: good slag formation, with a complete coating on the weld.

After the slag was removed, the surface appearance (SA) of the weld beads was evaluated. This was scored on a 1-10 basis, according to the following criteria:

1: weld bead totally defective;
2: weld bead with high occurrence of defects (more than six) and rough SA;
3: weld bead with high occurrence of defects (more than six) and SA appearance;
4: weld bead with an average occurrence of defects (from four to six) and rough SA,
5: weld bead with an average occurrence of defects (from four to six) and smooth SA;
6: weld bead with little occurrence of defects (one to three) and rough SA;
7: weld bead with little occurrence of defects (one to three) and smooth SA;
8: weld bead free from defects and rough SA;
9: weld bead free from defects and partially smooth SA and partially rough;
10: weld bead free from defects and smooth SA.

Figures 3 and 4 show some examples of the quality assessment of claddings.

(2) Calculation of the responses of productivity: to measure the variables of productivity, the carbon steel plates were weighed before and after the deposition of beads. Also, welding time was recorded. Thus, the fusion rate (FR), the deposition rate (DR), and process yield (Y) were calculated by the following expressions:

$$\text{Fusion rate: } \mathrm{FR} = \frac{l_w \cdot d_w}{t} \text{ (kg/h)} \quad \text{(Eq 1)}$$

which l_w is the length of flux cored wire consumed, calculated by:

$$l_w = W_f \cdot t \cdot 60 \text{ (m)} \quad \text{(Eq 2)}$$

where W_f is the wire feed rate (m/min); d_w the linear density of flux cored wire: 7.21×10^{-3} kg/m; and t is the welding time (h).

$$\text{Deposition rate: } \mathrm{DR} = \frac{(m_f - m_i)}{t} \text{ (kg/h)} \quad \text{(Eq 3)}$$

where m_i is the plate mass before welding (kg); m_f the plate mass after welding (kg); and t is the Welding time (h).

Table 3 Experimental matrix

	Parameters				Geometry				Productivity		Quality	
Test	W_f	V	S	N	W	P	R	D, %	DR	Y, %	SF	SA
1	−1	−1	−1	−1	11.19	1.37	2.63	26.44	2.718	89.74	3	7
2	1	−1	−1	−1	12.99	1.66	3.12	25.82	3.881	89.71	5	6
3	−1	1	−1	−1	12.70	1.69	2.50	31.49	2.699	89.14	3	10
4	1	1	−1	−1	15.05	1.98	2.78	31.25	3.871	89.47	3	…
5	−1	−1	1	−1	9.21	1.65	2.17	36.22	2.773	91.58	3	10
6	1	−1	1	−1	9.96	1.94	2.67	33.69	3.924	90.70	4	9
7	−1	1	1	−1	9.75	1.54	2.06	37.12	2.647	87.43	3	10
8	1	1	1	−1	11.51	2.18	2.42	41.08	3.822	88.36	3	8
9	−1	−1	−1	1	10.32	1.25	2.87	22.46	2.740	90.49	4	9
10	1	−1	−1	1	11.43	1.00	…	18.32	3.870	89.47	5	8
11	−1	1	−1	1	11.27	1.32	2.85	23.71	2.743	90.60	3	7
12	1	1	−1	1	13.34	1.10	3.18	21.96	3.885	89.81	4	4
13	−1	−1	1	1	7.99	1.11	2.55	24.96	2.847	94.03	3	9
14	1	−1	1	1	8.62	1.23	2.80	23.31	3.901	90.17	4	9
15	−1	1	1	1	8.48	1.37	2.36	28.77	2.832	93.52	3	10
16	1	1	1	1	10.84	1.64	2.60	30.19	3.969	91.74	3	7
17	−2	0	0	0	9.07	1.38	2.21	31.56	2.204	92.62	3	9
18	2	0	0	0	12.21	2.14	3.06	30.95	4.454	89.52	4	6
19	0	−2	0	0	9.42	1.20	3.03	22.84	3.324	90.41	4	9
20	0	2	0	0	11.69	1.86	2.46	35.58	3.311	90.04	3	8
21	0	0	−2	0	14.93	0.95	…	18.58	3.319	90.27	4	8
22	0	0	2	0	8.48	1.43	2.25	35.78	3.423	93.08	3	9
23	0	0	0	−2	11.73	2.18	2.61	40.44	3.242	88.15	3	8
24	0	0	0	2	9.22	1.28	2.89	24.16	3.385	92.05	3	8
25	0	0	0	0	10.82	1.71	2.60	31.05	3.421	93.04	3	8
26	0	0	0	0	10.93	1.72	2.59	31.67	3.380	91.91	3	8
27	0	0	0	0	10.74	1.62	2.65	30.88	3.402	92.51	3	7
28	0	0	0	0	10.61	1.80	2.50	32.83	3.382	91.98	3	8
29	0	0	0	0	10.64	1.49	2.62	29.99	3.388	92.15	3	7
30	0	0	0	0	10.59	1.49	2.61	31.09	3.398	92.40	3	7
31	0	0	0	0	10.57	1.50	2.56	31.02	3.404	92.58	3	8

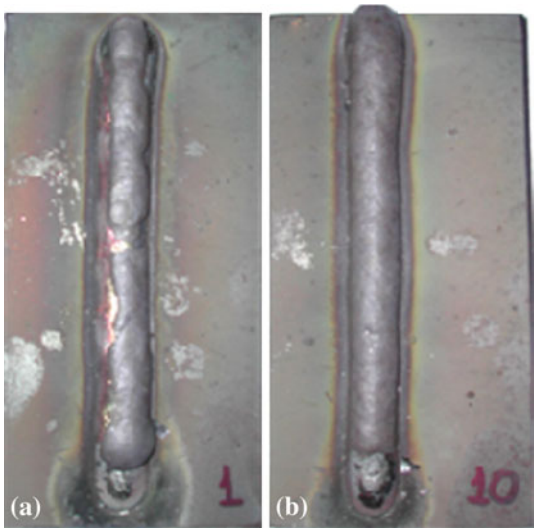

Fig. 3 Evaluation of slag formation: (a) Score 3 and (b) Score 5

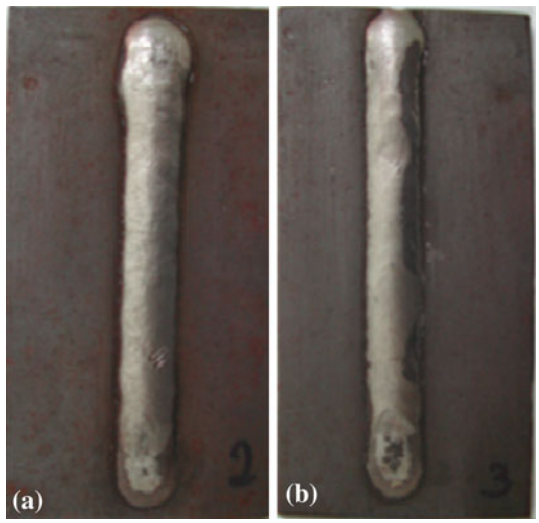

Fig. 4 Evaluation of surface appearance: (a) Score 6 and (b) Score 10

$$\text{Process yield: } Y = \frac{\text{DR}}{\text{FR}} \cdot 100\ (\%) \qquad \text{(Eq 4)}$$

(3) Measuring the weld bead geometry: The weld bead geometry was measured at four different points of the specimens. The beginning and the end of the process were discarded to get a better average of the responses. The samples were cut and their cross sections properly prepared, attacked with 4% nital, and photographed. Figure 5 shows the cross sections of two specimens after cutting, preparation, and attack. With the help of the image analysis software Analysis Doc®,

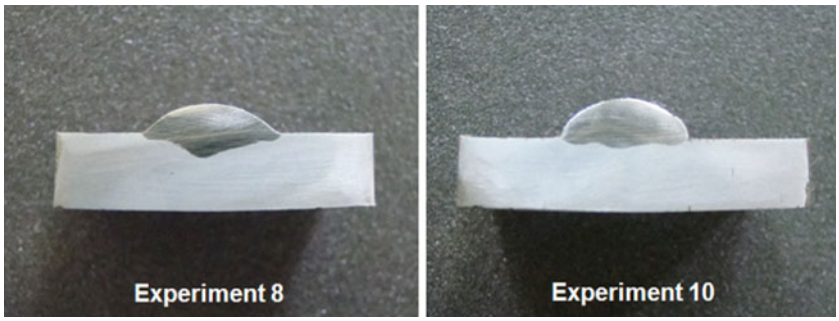

Fig. 5 Weld bead geometry after preparing the specimens

the weld bead dimensions were measured to obtain the bead width (W), penetration (P), reinforcement (R), area of penetration, and total area of the weld. The percentage of dilution (D) was then calculated by dividing the area of penetration by the total area.

After measuring all the responses of interest, these were assembled to create the experimental matrix shown in Table 3. Note that two data relating to the reinforcement (tests 10 and 21) and another referring to the surface appearance (test 2) were eliminated. These data were characterized as outliers. Their presence could have negatively influenced the estimation of mathematical models.

2.3 Mathematical Modelling of Responses of Interest

The second-order polynomial function developed for a response surface that relates a given response y with k input variables has the following format, described by Eq 5 (Ref 22):

$$y = \beta_0 + \sum_{i=1}^{k} \beta_i x_i + \sum_{i=1}^{k} \beta_{ii} x_i^2 + \sum \sum_{i<j} \beta_{ij} x_i x_j \quad \text{(Eq 5)}$$

where y is the response of interest; x_i is input parameters; β_0, β_i, β_{ii}, β_{ij} are the coefficients to be estimated; and k is the number of input parameters considered.

Considering the process discussed in this study, which investigates the effects of four parameters, Eq 5 can be rewritten as shown in Eq 6 below:

$$\begin{aligned} y = {} & \beta_0 + \beta_1 W_f + \beta_2 V + \beta_3 S + \beta_4 N + \beta_{11} W_f^2 + \beta_{22} V^2 \\ & + \beta_{33} S^2 + \beta_{44} N^2 + \beta_{12} W_f V + + \beta_{13} W_f S + \beta_{14} W_f N \\ & + \beta_{23} VS + \beta_{24} VN + \beta_{34} SN \end{aligned} \quad \text{(Eq 6)}$$

The statistical software Minitab® was employed to develop the mathematical models. It uses the ordinary least squares (OLS) method to obtain the coefficients related to the model. Table 4 presents the estimated coefficients for the complete quadratic models developed to the responses considered in this study.

The adequacy of the models was verified using analysis of variance (ANOVA), also made by Minitab®. Results of this analysis are found in Table 5. All developed models were adequate, since they had p-values less than 5% of significance. The results from ANOVA also indicated that, aside from the surface appearance, all the developed models showed good adjustments. The values of adj. R^2 were over 80%. As for superficial appearance, the adjustment obtained was 61.82%, considered a value not too good, but acceptable.

After the adequacies of the models were verified, these were reduced by removing insignificant terms. The criteria for removal were (1) increase in the adj. R^2 value, and (2) reduction in the variance of the models. Thus, the final models had the shapes described by Eq 7-14, while Table 6 shows the new adjustments obtained. The three digits on the coefficients were statistically defined as result of a previous study of repeatability and reproducibility.

$$\begin{aligned} W = {} & 10.640 + 0.797 W_f + 0.656 V - 1.451 S - 0.629 N \\ & + 0.270 S^2 + 0.266 W_f V - 0.114 W_f S - 0.102 VS \\ & + 0.067 SN \end{aligned} \quad \text{(Eq 7)}$$

$$\begin{aligned} P = {} & 1.639 + 0.122 W_f + 0.122 V + 0.093 S - 0.241 N \\ & + 0.025 W_f^2 - 0.032 V^2 - 0.118 S^2 + 0.034 W_f V \\ & + 0.076 W_f S - 0.100 W_f N \end{aligned} \quad \text{(Eq 8)}$$

$$\begin{aligned} R = {} & 2.597 + 0.191 W_f - 0.104 V - 0.223 S + 0.115 N \\ & + 0.034 V^2 + 0.019 S^2 + 0.036 N^2 - 0.030 W_f V \\ & - 0.023 W_f N \end{aligned} \quad \text{(Eq 9)}$$

$$\begin{aligned} D = {} & 0.310 - 0.003 W_f + 0.025 V + 0.037 S - 0.043 N \\ & - 0.007 V^2 - 0.012 S^2 + 0.008 W_f V + 0.005 W_f S \\ & - 0.004 W_f N - 0.008 SN \end{aligned} \quad \text{(Eq 10)}$$

$$\begin{aligned} \mathrm{DR} = {} & 3.396 + 0.568 W_f - 0.009 V + 0.021 S + 0.031 N \\ & - 0.019 W_f^2 - 0.022 V^2 - 0.008 S^2 - 0.023 N^2 \\ & + 0.008 W_f V - 0.006 W_f S - 0.012 W_f N - 0.010 VS \\ & + 0.020 VN + 0.019 SN \end{aligned} \quad \text{(Eq 11)}$$

$$\begin{aligned} Y = {} & 0.924 - 0.006 W_f - 0.003 V + 0.006 S + 0.009 N \\ & - 0.004 W_f^2 - 0.006 V^2 - 0.002 S^2 - 0.006 N^2 \\ & + 0.003 W_f V - 0.003 W_f S - 0.005 W_f N - 0.003 VS \\ & + 0.006 VN + 0.006 SN \end{aligned} \quad \text{(Eq 12)}$$

$$\begin{aligned} \mathrm{SF} = {} & 3.021 + 0.333 W_f - 0.333 V - 0.250 S + 0.083 N \\ & + 0.144 W_f^2 + 0.144 V^2 + 0.144 S^2 - 0.250 W_f V \\ & - 0.125 W_f S + 0.125 VS - 0.125 SN \end{aligned} \quad \text{(Eq 13)}$$

$$\begin{aligned} \mathrm{SA} = {} & 7.644 - 0.855 W_f - 0.272 V + 0.689 S - 0.145 N \\ & + 0.219 V^2 + 0.219 S^2 - 0.533 W_f V - 0.592 VN \end{aligned} \quad \text{(Eq 14)}$$

Finally, the response surfaces relating the process parameters with the responses of geometry, productivity, and quality of the claddings were plotted using the software Minitab®. How-

Table 4 Estimated coefficients for complete quadratic models

Coefficient	Responses							
	W	*P*	*R*	*D*	DR	*Y*	SF	SA
Constant	**10.6996**	**1.6192**	**2.5898**	**0.3122**	**3.3964**	**0.9237**	**3.0000**	**7.5714**
β_1	**0.7967**	**0.1221**	**0.1921**	−0.0028	**0.5676**	**−0.0055**	**0.3333**	**−0.8792**
β_2	**0.6555**	**0.1220**	**−0.1051**	**0.0249**	−0.0088	−0.0027	**−0.3333**	−0.2958
β_3	**−1.4507**	**0.0934**	**−0.2230**	**0.0368**	**0.0214**	**0.0061**	**−0.2500**	**0.7125**
β_4	**−0.6290**	**−0.2408**	**0.1155**	**−0.0425**	**0.0308**	**0.0090**	0.0833	−0.1208
β_{11}	−0.0033	0.0266	0.0069	−0.0023	**−0.0190**	**−0.0039**	**0.1458**	−0.0293
β_{22}	−0.0240	−0.0300	**0.0346**	**−0.0074**	**−0.0218**	**−0.0060**	**0.1458**	0.2207
β_{33}	**0.2637**	**−0.1161**	0.0196	**−0.0125**	−0.0084	−0.0024	**0.1458**	0.2207
β_{44}	−0.0440	0.0190	**0.0368**	0.0003	**−0.0229**	**−0.0063**	0.0208	0.0957
β_{12}	**0.2663**	0.0337	−0.0309	0.0077	0.0080	0.0028	**−0.2500**	**−0.5688**
β_{13}	−0.1137	**0.0757**	−0.0146	0.0050	−0.0057	−0.0026	**−0.1250**	0.1938
β_{14}	−0.0308	**−0.0998**	−0.0219	−0.0042	**−0.0124**	**−0.0049**	0.0000	0.0687
β_{23}	−0.1023	0.0002	−0.0049	0.0023	−0.0103	−0.0032	**0.1250**	0.0687
β_{24}	−0.0064	0.0048	0.0148	−0.0020	**0.0204**	**0.0055**	0.0000	**−0.5563**
β_{34}	0.0665	0.0045	−.0144	−0.0077	**0.0195**	**0.0057**	**−0.1250**	−0.0688

Coefficients in bold indicate significant terms

Table 5 Analysis of variance

Response	Degrees of freedom		Adj. sum-of-squares		Adj. mean-square		*F*-ratio	*P*	Adj. R^2, %
	Regression	Residual	Regression	Residual	Regression	Residual			
W	14	16	89.355	0.975	6.383	0.061	104.73	0.000	97.98
P	14	16	3.054	0.300	0.218	0.019	11.64	0.000	83.24
R	14	14	2.067	0.088	0.148	0.006	23.58	0.000	91.86
D	14	16	0.099	0.004	0.007	0.000	31.49	0.000	93.43
DR	14	16	7.817	0.008	0.558	0.000	1131.65	0.000	99.81
Y	14	16	0.008	0.001	0.001	0.000	12.92	0.000	84.77
SF	14	16	10.263	0.833	0.733	0.052	14.08	0.000	85.92
SA	14	15	42.507	10.460	3.036	0.697	4.35	0.004	61.82

Tabulated values of *F*: $F_{95\%}$ (14, 16) = 2.37; $F_{95\%}$ (14, 15) = 2.42; $F_{95\%}$ (14, 14) = 2.48

ever, such surfaces will be discussed in more detail later along with the analysis of the interaction effects of parameters.

3. Results and Discussion

The results found in Table 6 indicate that the final models developed can be characterized as being quite reliable. All models, aside from the surface appearance, presented adjustments in excess of 84%. Nevertheless, the reduction procedure improved the adjustment of the surface appearance from 61.82 to 70.34%, considered a satisfactory adjustment.

Having developed the final models, it was possible to analyze how changes in the input parameters affected the process responses. By varying one parameter at a time, its influence over the responses could be studied. This clarified important information about the process in question. Thus, in this section, the different influences of FCAW parameters on weld bead geometry, productivity, and quality of stainless steel claddings are discussed.

3.1 Main Effects of Parameters on the Weld Bead Geometry

Figure 6 presents the main effects on the bead width of claddings, showing how this response is influenced by FCAW parameters.

Similar figures could be obtained for penetration, reinforcement, and dilution. The results in Fig. 6 indicates that increasing the wire feed rate and voltage and decreasing the welding speed and CTWD result in larger bead widths. This occurs because the increase in wire feed rate causes a rise in the welding current. The amount of material deposited increases, resulting in higher weld bead dimensions. Likewise, increased voltages are positively correlated with increased width, i.e., the higher the voltage the greater the bead width and vice versa. As for welding speed, lower speeds cause, for each unit of time, greater amounts of material to be deposited in a given length, resulting in higher dimensions. For the CTWD, an increase in distance increases the length and the Joule effect in the wire, causing a drop in heat in the weld pool. This fall in heat reduces the weld bead dimensions. Thus, smaller distances produce greater bead widths.

Similarly, the results for penetration showed that a decrease in wire feed rate and voltage result in lower penetration. This is

Table 6 Comparison between the adjustment of the complete models and final models

	Adj. R^2, %		Variance	
Response	Complete model	Final model	Complete model	Final model
W	97.98	98.33	0.2469	0.2244
P	83.24	86.10	0.1369	0.1247
R	91.86	93.20	0.0791	0.0723
D	93.43	94.30	0.0150	0.0140
DR	99.81	99.81	0.0222	0.0222
Y	84.77	84.77	0.0065	0.0065
SF	85.92	87.97	0.2282	0.2110
SA	61.82	70.34	0.8351	0.7361

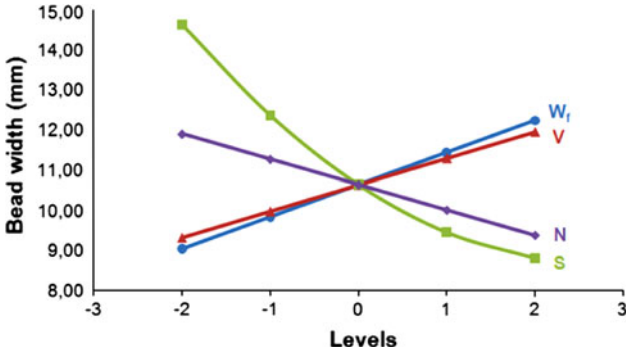

Fig. 6 Influence of parameters on the bead width

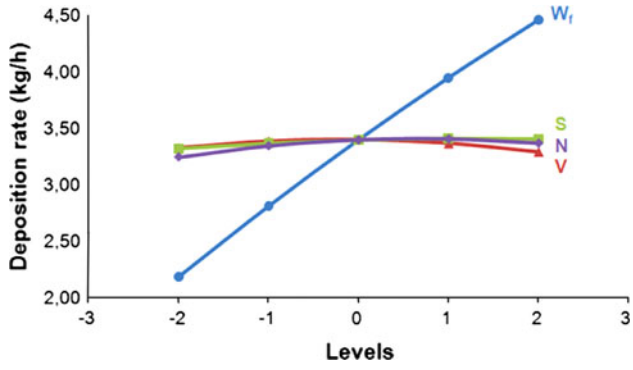

Fig. 7 Influence of parameters on the deposition rate

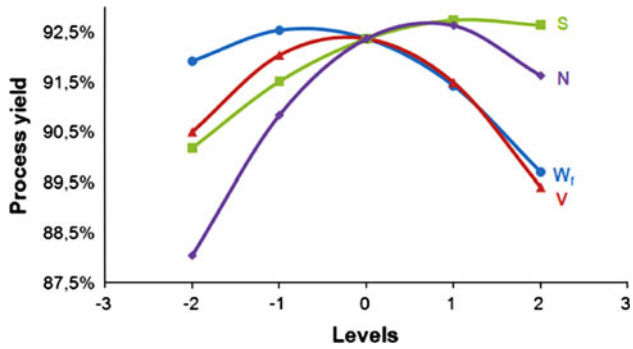

Fig. 8 Influence of parameters on the process yield

due to the lower current and welding energy brought about by reducing these parameters. For the CTWD, longer distances increased the Joule heating of the wire and decreased the penetration. For this response, the welding speed made a curvature point, reaching a maximum penetration at a welding speed of 44 cm/min. Lower values of penetration were observed at extreme welding speeds.

For reinforcement, it was observed that its increasing is related to low voltages, low welding speeds, high wire feed rates, and high CTWD. Reinforcement is inversely related to voltage. Lower voltages result in stronger reinforcements and higher voltages result in weaker reinforcements. For the welding speed, lower speeds cause greater deposition of material per unit of time, which leads to larger weld beads. Obtaining greater reinforcements at higher wire feed rates is also related to increasing the welding current and the amount of material deposited. Increasing the CTWD lowers the heat in the weld pool. The molten metal consequently has insufficient energy to penetrate in the base metal. Hence, the filler metal, unable to penetrate in the piece, just accumulates on the base metal, increasing the reinforcement.

The results for dilution showed that low voltages, low welding speeds, and high CTWD produced lower levels of dilution. For this response, wire feed rate is a parameter with little impact. It was also observed that low voltages and low welding speeds produce low penetration and high reinforcement. Therefore, the reinforcement area increases and the penetration area decreases, resulting in low dilution percentages. The same reasoning applies to the CTWD. Under conditions of greater distances, low penetration and high reinforcements were observed, leading to decreased dilution.

3.2 Main Effects of Parameters on Productivity

The influences of parameters on the deposition rate and process yield are shown in Fig. 7 and 8, respectively.

Figure 7 shows that only wire feed rate was characterized as a significant parameter for the deposition rate. Higher wire feed rates deposit a greater amount of material on the base metal. This explains why the deposition rate goes up at higher wire feed rate levels.

The effects of the parameters on the process yield (Fig. 8) showed that each curve presented a curvature point. That is, a maximum yield was recorded for each parameter. The yield in a welding process is related to loss of filler metal caused by spatter. Therefore, CTWD was the most sensitive to such loss, followed by voltage, wire feed rate, and welding speed. In addition, Fig. 8 suggests an overall yield for the process of around 92%, located close to the center points.

3.3 Main Effects of Parameters on the Quality

Analyzing how the parameters influence surface quality of claddings is relevant in monitoring poor slag formation and occurrence of defects. Poor slag formation results in marks on the side of the welds, and defects are detrimental to the properties of claddings.

Within this context, Fig. 9 shows that better slag formation can be achieved with low voltage levels, low welding speeds, and high wire feed rates. The CTWD was characterized as an insignificant parameter. Higher wire feed rates deposit larger quantities of material. Thus, the amount of flux deposited—the material in the wire responsible for slag formation—is also higher, causing slag to be formed with few flaws. At low

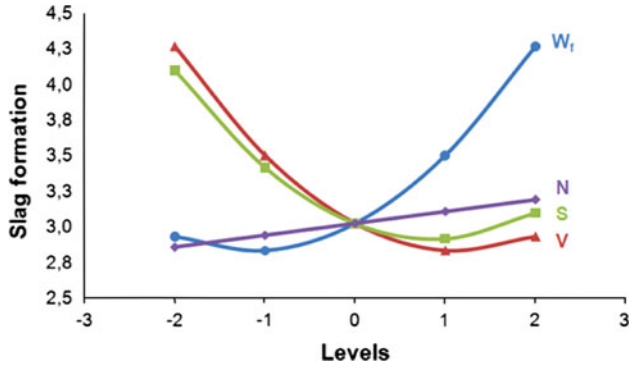

Fig. 9 Influence of parameters on the slag formation

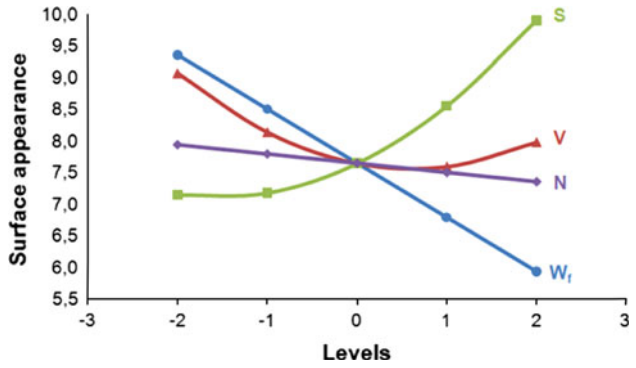

Fig. 10 Influence of parameters on the surface appearance

welding speeds, the weld pool is on a given length of base metal for longer duration. Thus, it takes longer time to form slag, helping in turning out a better coating. As for voltage, low voltages help form a weld bead with greater convexity (small bead widths and larger reinforcements). This geometric feature is conducive to a better slag coating.

Considering the surface appearance (Fig. 10), it was found that defect-free weld beads were obtained at low wire feed rates, low voltages, and high welding speeds. The insignificant parameter for this response was, again, the CTWD. High wire feed rates, high voltages, and low welding speeds raised the welding energy and the heat imposed on the base metal. Consequently, the material's cooling rate went up, making it solidify in an uncontrolled manner. Such uncontrolled solidifying favors the formation of defects. This explains why some defects, mainly elongated superficial porosities, were observed at high wire feed rates and low welding speeds. Figure 10 shows that in spite of rising voltages helping to increase the material's heat input, the variation of this parameter fluctuated within a defect-free region (grades above 7.5). Therefore, it can be stated that changing the voltage did not damage the surface quality of the claddings.

3.4 Interaction Effects of Parameters on the Weld Bead Geometry

Table 4 shows that several interactions between the parameters were found to be significant. This means that the combined effect of these parameters significantly influences the process's outcomes. Such interactions were analyzed using the response surfaces developed in the end of item 2.3.

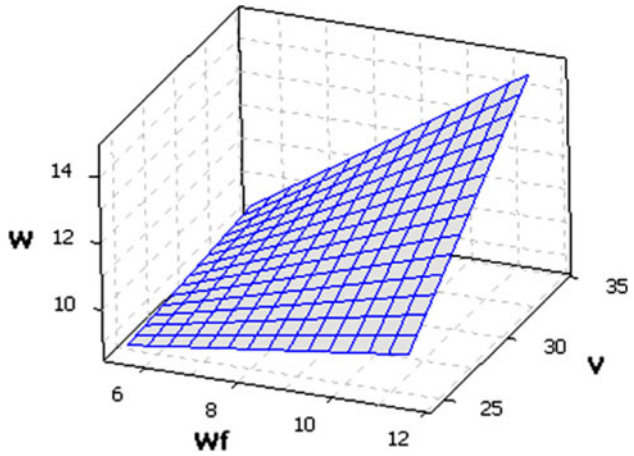

Fig. 11 Interaction between wire feed rate and voltage on bead width (S = 40 cm/min; N = 20 mm)

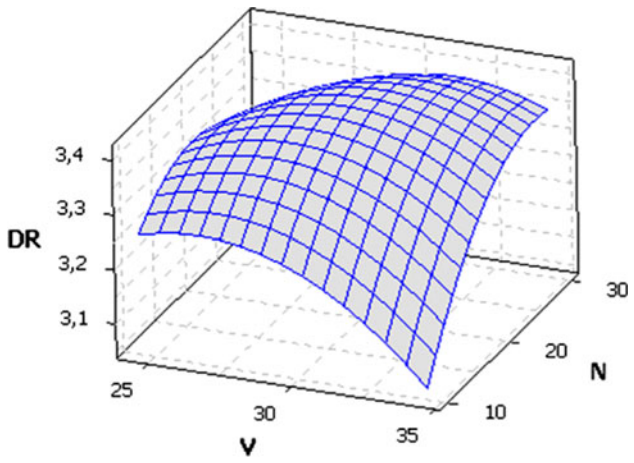

Fig. 12 Interaction between voltage and CTWD on deposition rate (W_f = 8.5 m/min; S = 40 cm/min)

Figure 11 shows the combined effect of voltage and wire feed rate on bead width. As presented earlier, both parameters influence this result. Figure 11, however, shows that also significant is the interaction between these two parameters. Thus, increasing the wire feed rate while increasing the voltage widens the weld bead considerably. Similar figures, representing other interaction effects on the weld bead geometry, can be plotted in the same way of Fig. 11. Nevertheless, these graphics are not depicted here.

3.5 Interaction Effects of Parameters on Productivity

Figures 12 and 13 show the effects of interactions on the productivity of the cladding process. Considering the deposition rate, Fig. 12 illustrates one of the most important aspects related to interaction analysis. Here, two non-significant parameters, working together, generated significant effects on this response. As previously discussed, voltage, welding speed, and CTWD, when taken individually, did little affect deposition rate. Yet the interaction of these parameters generated significant effects. The deposition rate increased significantly for voltages near 32 V and CTWD of about 25 mm. Figure 13 illustrates an interaction effect on the process yield, to which similar analysis can be attributed.

3.6 Interaction Effects on the Quality

Figures 14 and 15 show how the interactions between parameters affect the slag formation and surface appearance. We know that a weak influential parameter on these responses was CTWD. However, the interaction of this parameter with other variables resulted in significant increases to the cladding quality. Increasing the CTWD at lower welding speeds and lower voltages favored better slag formation and defect-free weld beads.

3.7 Pareto Frontiers

The graphical analysis of the previous sections points out that the several responses of the stainless steel cladding process present conflicts of interest. In other words, the set of welding parameters that provides the best result for a given characteristic is not the same that optimizes the others. This information is also observed in Fig. 16, which represents the Pareto frontier developed for the responses bead width and dilution. From this figure, it is seen that the process presents different optimal sets when the responses are optimized with greater or lesser degree of importance.

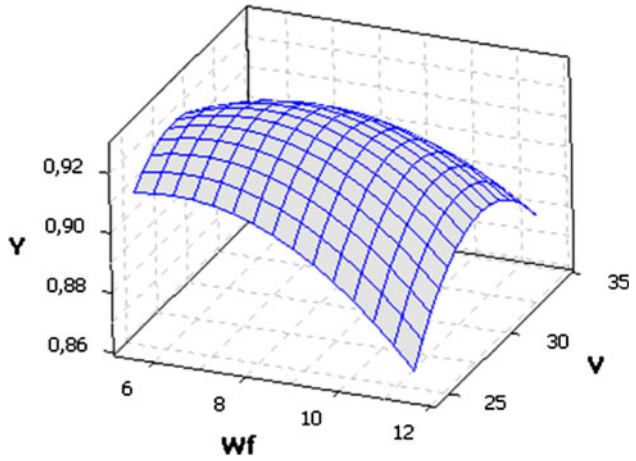

Fig. 13 Interaction between wire feed rate and voltage on process yield (S = 40 cm/min; N = 20 mm)

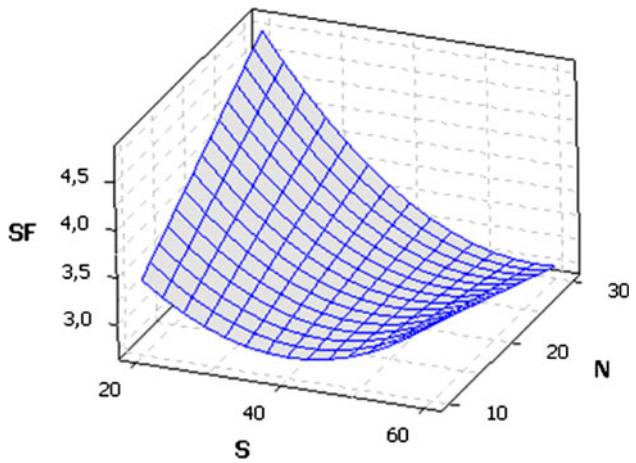

Fig. 14 Interaction between welding speed and CTWD on slag formation (W_f = 8.5 m/min; V = 29.5 V)

In a similar way, Fig. 17 illustrates the trade-off between quality and productivity for this cladding process, showing that the obtaining of the best quality implies in loss of productivity and vice versa.

The development of Pareto frontiers was made by solving the following expression:

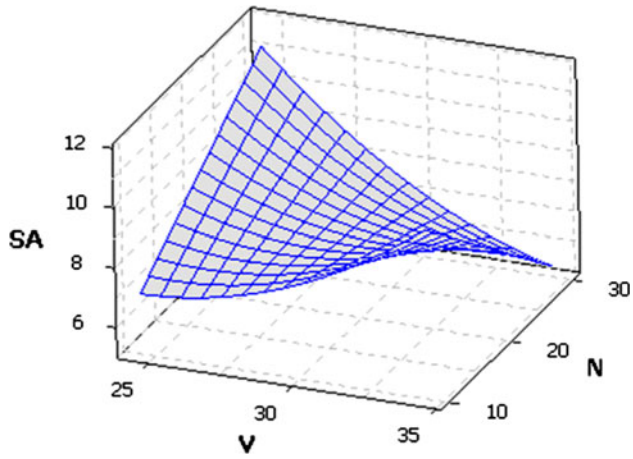

Fig. 15 Interaction between voltage and CTWD on surface appearance (W_f = 8.5 m/min; S = 40 cm/min)

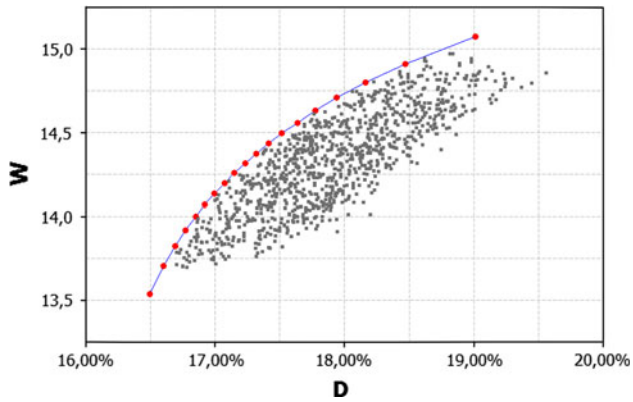

Fig. 16 Pareto frontier for bead width vs. dilution

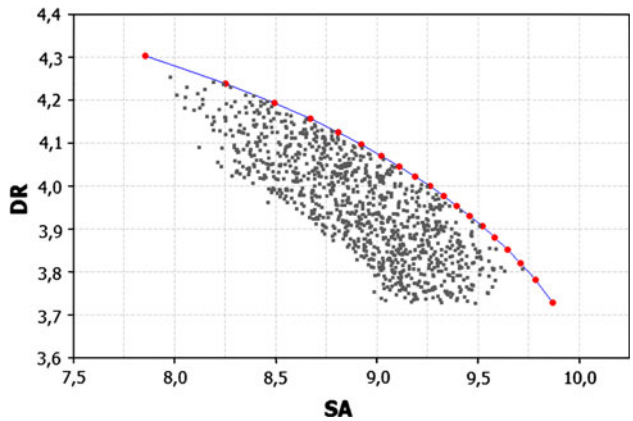

Fig. 17 Pareto frontier for deposition rate vs. surface appearance

$$\text{Min } F(\mathbf{x}) = w \cdot \left(\frac{T_{Y_1} - Y_1}{T_{Y_1}}\right)^2 + (1-w) \cdot \left(\frac{T_{Y_2} - Y_2}{T_{Y_2}}\right)^2 \quad \text{(Eq 15)}$$

$$\text{Subject to: } \mathbf{x}^{\mathbf{T}}\mathbf{x} \leq \alpha^2 \quad \text{(Eq 16)}$$

where $F(\mathbf{x})$ is the agglutination function of the objective functions; Y_i the RSM models of the responses of interest; T_{Y_i} the specified targets for the responses of interest; w the weight or degree of importance of the responses of interest; and $\mathbf{x}^{\mathbf{T}}\mathbf{x} \leq \alpha^2$ is the spherical constraint for the experimental region, with $\alpha = 2.0$.

In Eq 15, the targets were fixed after the individual optimization of the RSM models, with minimization for dilution and maximization for bead width, deposition rate, and surface appearance. The weights w varied from 0.05 to 0.95, with increments of 0.05. In both Fig. 16 and 17, the cloud of gray points represents dominated solutions by the optimal-Pareto solutions which determine the frontier.

Once conflicts of interest were identified by the analysis presented in sections 3.1-3.6 and confirmed by Pareto frontiers, it becomes interesting to apply multi-objective optimization techniques on this process, to find a set of welding parameters that provides a global optimal solution for all process outcomes. However, as this topic was not the main objective of this study, it will be reserved for future researches.

4. Conclusions

From the results shown in previous sections the following conclusions can be drawn:

1. The mathematical models developed presented high adjustments and can be characterized as expressions of great reliability. Apart from surface appearance, all models were adjusted over 84%. For surface appearance, the adjustment obtained was 70.34%, considered a satisfactory value.
2. All parameters analyzed had significant influence on the cladding process outcomes. However, the degrees of importance among them varied depending on the response of interest.
3. As for the desired geometry of the cladding process, larger bead widths may be obtained by employing high wire feed rates, high voltages, low welding speeds, and low CTWD.
4. Minor penetrations are achieved by decreasing the wire feed rate, voltage and welding speed and by increasing the CTWD. When the welding speed was about 44 cm/min the result was a maximum penetration.
5. Increased reinforcement is obtained by increasing the wire feed rate and CTWD and by decreasing the voltage and welding speed.
6. For dilution, low percentages are achieved at low voltages, low welding speeds and high CTWD. The wire feed rate yielded little influence on this response.
7. Better productivity is related to higher deposition rates and higher process yields. Increasing the deposition rate depends only on increasing the wire feed rate. Voltage, welding speed, and CTWD had no significant influence on this response. The process yield curves identified a maximum value for each parameter, suggesting for the process an overall yield of around 92%.
8. The CTWD exerted little influence on surface quality. Defect-free weld beads are produced from increasing welding speed, and reducing wire feed rate and voltage. Better slag formation is produced at high wire feed rates, low voltages, and low welding speeds.
9. An important element for the process control is to analyze the interactions between parameters. A parameter with little influence on its own can, through interaction with another parameter, produce significant effects. There are lots of second-order interactions that affect the responses, as seen on Table 4.
10. The existence of conflicts of interest, as identified by previous findings and confirmed by Pareto frontiers, suggests, as theme for future studies, the application of multi-objective optimization methods on this problem. The aim is to achieve a global solution that addresses all the process outcomes at the same time.

References

1. A.L. Phillips, *Welding Handbook: Special Welding Processes and Cutting*, 5th ed., Macmillan, London, 1965
2. N. Murugan and R.S. Parmar, Stainless Steel Cladding Deposited by Automatic Gas Metal Arc Welding, *Weld. J.*, 1997, **76**, p 391s–403s
3. N. Murugan and R.S. Parmar, Effects of MIG Process Parameters on the Geometry of the Bead in the Automatic Surfacing of Stainless Steel, *J. Mater. Process. Technol.*, 1994, **41**, p 381–398
4. P.K. Palani and N. Murugan, Development of Mathematical Models for Prediction of Weld Bead Geometry in Cladding by Flux Cored Arc Welding, *Int. J. Adv. Manuf. Technol.*, 2006, **30**, p 669–676
5. P.K. Palani and N. Murugan, Optimization of Weld Bead Geometry for Stainless Steel Claddings Deposited by FCAW, *J. Mater. Process. Technol.*, 2007, **190**, p 291–299
6. T. Kannan and N. Murugan, Effect of Flux Cored Arc Welding Process Parameters on Duplex Stainless Steel Clad Quality, *J. Mater. Process. Technol.*, 2006, **176**, p 230–239
7. A.S. Shahi and S. Pandey, Prediction of Dilution in GMA and UGMA Stainless Steel Single Layer Cladding Using Response Surface Methodology, *Sci. Technol. Weld. Join.*, 2006, **11**, p 634–640
8. V. Balasubramanian, A.K. Lakshminarayanan, R. Varahamoorthy, and S. Babu, Application of Response Surface Methodology to Prediction of Dilution in Plasma Transferred Arc Hardfacing of Stainless Steel on Carbon Steel, *Int. J. Iron Steel Res.*, 2009, **16**, p 44–53
9. A.S. Shahi and S. Pandey, Modelling of the Effects of Welding Conditions on Dilution of Stainless Steel Claddings Produced by Gas Metal Arc Welding Procedures, *J. Mater. Process. Technol.*, 2008, **196**, p 339–344
10. T. Ishida, Formation of Stainless Steel Layer on Mild Steel by Welding Arc Cladding, *J. Mater. Sci.*, 1991, **26**, p 6431–6435
11. U.D. Mallya and H.S. Srinivas, Effect of Magnetic Steering of the Arc on Clad Quality in Submerged Arc Strip Cladding, *Weld. J.*, 1993, **72**, p 289s–293s
12. R. Li, M.G.S. Ferreira, M.A. Anjos, and R. Vilar, Localized Corrosion of Laser Surface Cladded UNS S31254 Superaustenitic Stainless Steel on Mild Steel, *Surf. Coat. Technol.*, 1996, **88**, p 90–95
13. R. Li, M.G.S. Ferreira, M.A. Anjos, and R. Vilar, Localized Corrosion Performance of Laser Surface Cladded UNS S44700 Superferritic Stainless Steel on Mild Steel, *Surf. Coat. Technol.*, 1996, **88**, p 96–102
14. M.A. Anjos, R. Vilar, and Y.Y. Qiu, Laser Cladding of ASTM S31254 Stainless Steel on a Plain Carbon Steel Substrate, *Surf. Coat. Technol.*, 1997, **92**, p 142–149
15. R. Rajeev, I. Samajdar, R. Raman, C.S. Harendranath, and G.B. Kale, Origin of Hard and Soft Zone Formation During Cladding of Austenitic/Duplex Stainless Steel on Plain Carbon Steel, *Mater. Sci. Technol.*, 2001, **17**, p 1005–1011
16. C.K. Sha and H.L. Tsai, Hardfacing Characteristics of S42000 Stainless Steel by Using CO2 Laser, *J. Mater. Eng. Perform.*, 2001, **10**, p 37–41

17. J.D. Majumdar, A. Pinkerton, Z. Liu, I. Manna, and L. Li, Mechanical and Electrochemical Properties of Multiple-Layer Diode Laser Cladding of 316L Stainless Steel, *Appl. Surf. Sci.*, 2005, **247**, p 373–377
18. I.C. Kuo, C.P. Chou, C.F. Tseng, and I.K. Lee, Submerged Arc Stainless Steel Strip Cladding—Effect of Post-Weld Heat Treatment on Thermal Fatigue Resistance, *J. Mater. Eng. Perform.*, 2009, **18**, p 154–161
19. A.S. Shahi and S. Pandey, Effect of Auxiliary Preheating of the Filler Wire on Quality of Gas Metal Arc Stainless Steel Claddings, *J. Mater. Eng. Perform.*, 2008, **17**, p 30–36
20. Y.S. Tarng, S.C. Juang, and C.H. Chang, The Use of Grey-Based Taguchi Methods to Determine Submerged Arc Welding Process Parameters in Hardfacing, *J. Mater. Process. Technol.*, 2002, **128**, p 1–6
21. L. Jeffus, *Welding: Principles and Applications*, 5th ed., Thomson, Clifton Park, NY, 2003
22. D.C. Montgomery, *Design and Analysis of Experiments*, 6th ed., Wiley, New York, 2005
23. A. Jeang, Robust Cutting Parameters Optimization for Production Time via Computer Experiment, *Appl. Math. Model.*, 2010 (in press), doi: 10.1016/j.apm.2010.09.014
24. S.S. Habib, Study of the Parameters in Electrical Discharge Machining Through Response Surface Methodology Approach, *Appl. Math. Model.*, 2009, **33**, p 4397–4407